Go-sha-jinki-Gan (GJG) ameliorates allodynia in chronic constriction injury model mice via suppression of TNF-α expression in the spinal cord

Miho Nakanishi, MD[1], Aya Nakae, MD, PhD[2], Yuki Kishida, MD, PhD[1], Kousuke Baba, MD, PhD[1], Noriko Sakashita, MS[1], Masahiko Shibata, MD, PhD[3], Hideki Yoshikawa, MD, PhD[4] and Keisuke Hagihara, MD, PhD[1]

Abstract

Background: Alternative medicine is noted for its clinical effect and minimal invasiveness in the treatment of neuropathic pain. Go-sha-jinki-Gan, a traditional Japanese herbal medicine, has been used for meralgia and numbness in elderly patients. However, the exact mechanism of GJG is unclear. This study aimed to investigate the molecular mechanism of the analgesic effect of GJG in a chronic constriction injury model.

Results: GJG significantly reduced allodynia and hyperalgesia from the early phase (von Frey test, $p < 0.0001$; cold-plate test, $p < 0.0001$; hot-plate test $p = 0.011$; two-way repeated measures ANOVA). Immunohistochemistry and Western blot analysis revealed that GJG decreased the expression of Iba1 and tumor necrosis factor-α in the spinal cord. Double staining immunohistochemistry showed that most of the tumor necrosis factor-α was co-expressed in Iba1-positive cells at day 3 post-operation. GJG decreased the phosphorylation of p38 in the ipsilateral dorsal horn. Moreover, intrathecal injection of tumor necrosis factor-α opposed the anti-allodynic effect of GJG in the cold-plate test.

Conclusions: Our data suggest that GJG ameliorates allodynia in chronic constriction injury model mice via suppression of tumor necrosis factor-α expression derived from activated microglia. GJG is a promising drug for the treatment of neuropathic pain induced by neuro-inflammation.

Background

Neuropathic pain (NP) is a serious health issue, negatively affecting quality of life and resulting in increased health care costs.[1] NP can result from disorders of the central or peripheral nervous system. Disorders giving rise to central NP include stroke, multiple sclerosis, and spinal cord injuries.[2] On the other hand, peripheral NP is caused by chemotherapy, HIV therapy, and diabetic mellitus.[3] However, the treatment strategy for NP remains controversial. A meta-analysis of pharmacotherapy for NP showed that effects of first-line drugs, e.g., serotonin-noradrenaline reuptake inhibitors and gabapentin, are moderate.[4] Drowsiness, nausea, and dizziness are reported side effects of these drugs[4,5] Moreover, NP

[1]Department of Kampo Medicine, Graduate School of Medicine, Osaka University, Suita, Japan
[2]Immunology Frontier Research Center, Laboratory of Brain-Immune Interaction, Osaka University, Suita, Japan
[3]Department of Pain Medicine, Graduate School of Medicine, Osaka University, Suita, Japan
[4]Department of Orthopaedic Surgery, Graduate School of Medicine, Osaka University, Suita, Japan

Corresponding author:
Keisuke Hagihara, Department of Kampo Medicine, Graduate School of Medicine, Osaka University, 2-2 Yamadaoka, Osaka, Suita 565-0871, Japan.
Email: hagihara.keisuke@gmail.com

is often refractory to conventional pain therapies.[6] Furthermore, finding a balanced approach to pain management in elderly patients can be challenging[7,8] because adverse events tend to occur in this patient group with medical treatment.[7] To date, no ideal treatment for NP has been established.[9] In view of the above issues, the development of novel therapies for NP is highly anticipated.

Recently, alternative medicine, which is minimally invasive, has attracted attention.[10,11] In Japan, traditional herbal medicine is known as Kampo medicine. Kampo formulas have been approved as drugs for clinical use by Japan's National Health Insurance Program. Go-sha-jinki-Gan (GJG) (Figure 1), a Kampo medicine that is composed of 10 herbal drugs in fixed proportions,[12] has been widely used in the treatment of meralgia, lower back pain, numbness, and neuropathy in elderly patients. Several clinical studies have demonstrated the efficacy of GJG in the treatment of peripheral neuropathy induced by anti-cancer drugs[13–16] as well as diabetic neuropathy.[17,18] No severe adverse events were observed in these clinical studies of GJG. In Japan, GJG is commonly used for the treatment of NP.

Microglia in the spinal cord are key cellular intermediaries in the development of NP.[19] Also, the cytokine tumor necrosis factor (TNF)-α has been established as a principal mediator in pro-inflammatory processes.[20] TNF-α secreted from activated microglia plays a pivotal role in central and peripheral mechanisms of NP.[21] The activation of TNF receptors results in p38 mitogen-activated protein kinase (MAPK) activation in spinal microglia,[22] which accelerates the inflammatory process in the spinal cord.[23] The molecular mechanism of GJG in NP has been investigated. GJG inhibits chronic phase chemotherapy-induced neuropathy via alteration of transient receptor potential (TRP), channel function,[6,24,25] and streptozocin-induced diabetic neuropathy via increased nitric oxide production[18] However, the effect of GJG on the pro-inflammatory process, especially on TNF-α expression, remains unclear.

Recently, we demonstrated that GJG protects against sarcopenia in senescence-accelerated mice. Sarcopenia is the age-associated weakening and loss of volume in muscle. In our study, GJG improved mitochondrial function and insulin/insulin-like growth factor-1 signal transduction. GJG also decreased the expression of TNF-α in muscle. In addition, TNF-α has been strongly
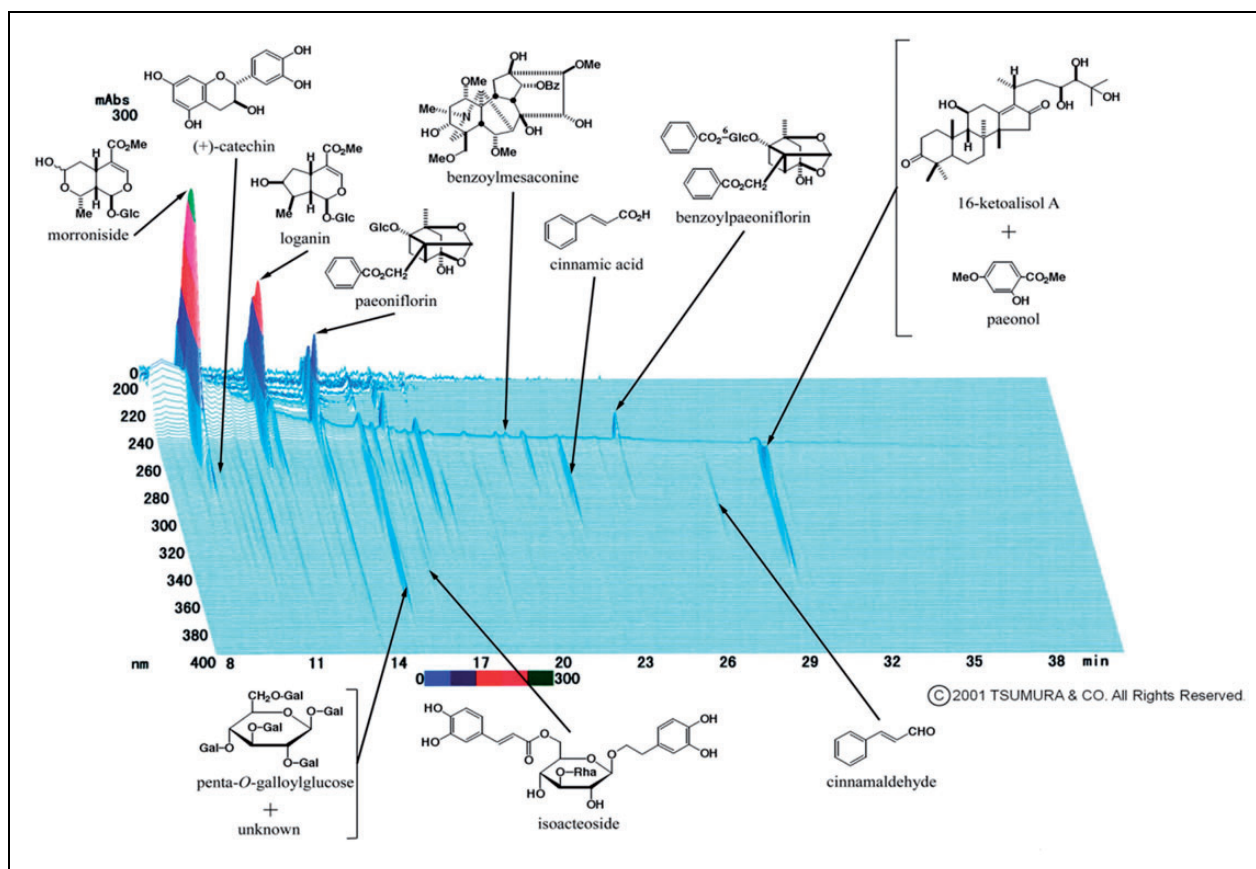

Figure 1. 3D-HPLC analysis of GJG.

implicated in the pathogenesis of NP described above. Thus, we propose that GJG inhibits NP via the suppression of TNF-α expression in the spinal cord. The chronic constriction injury (CCI) mouse model has been employed as a typical NP model. The purpose of this study was to determine whether GJG attenuates CCI-induced allodynia and hyperalgesia using behavioral tests. Next, we investigated the molecular mechanism of the analgesic effect of GJG in a CCI mouse model, including the involvement of TNF-α. Our data suggest that GJG effectively reduced NP in CCI model mice via a reduction in TNF-α expression in the dorsal horn. These results indicate that GJG is a promising drug for the treatment of NP.

Methods

Preparation of GJG extracts

GJG (extract granules in powdered form) was manufactured by Tsumura & Co. (Tokyo, Japan) according to Japanese and International manufacturing guidelines. GJG is a standardized prescription agent produced using 10 crude drugs. For use in humans, a daily dose of the study medication (7.5 g) contains 4.5 g of a spray-dried mixed extract made from the following crude drugs: 5 g *Rehmanniae radix* (*Rehmannia glutinosa* Liboschitz); 3 g each *Achyranthis radix* (*Achyranthes bidentage* Blume), *Corni fructus* (Cornus of ficinalis Sieb. et Zucc), *Dioscoreae rhizoma* (*Dioscorea batatas* Decaisne), *Plantaginis semen* (*Plantago asiatica*), *Alismatis rhizoma* (*Alisma orientale* Juzep), Hoelen (*Poria cocos* Wolf) and *Moutan cortex* (*Paeonia suffruti-cosa* Andrews); and 1 g each *Cinnamomi cortex* (*Cinnamomum cassia* Blume) and heat-processed Aconite tuber (*Aconitum carmichaelii* Debeaux) powder. A 3D high-performance liquid chromatography (HPLC) profile of GJG is shown in Figure 1.

Animals

C57BL/6J male mice, aged five weeks, were purchased from Charles River Japan (Tokyo, Japan) and were acclimatized for one week before experiments. All mice were housed under specific pathogen-free conditions and were given free access to food and water under a standard 12-h light/dark cycle (lights on 08:00–20:00) and regulated ambient temperature of $22 \pm 2^\circ$C. The mice were randomly divided into four groups: Sham group, GJG-treated Sham group, CCI group, and GJG-treated CCI group. All mice underwent the Sham or CCI operation and were fed a normal diet (powdered mouse diet consisting of 23% crude protein (w/w), 5% crude fat, 5.8% crude ash, 2.8% crude fiber, and 55.3% nitrogen-free extract and mineral mixture from Oriental Yeast

Co., Ltd. (Tokyo, Japan)) with or without 4% (w/w) GJG. Parameters such as general condition, food intake, and body weight were recorded for all mice at several time points (1 day before surgery, and then 7, 14, 21, and 28 days after surgery). All surgical and experimental protocols in this study were reviewed and approved by the Institutional Animal Care and Use Committee of Osaka University Graduate School of Medicine and were carried out in accordance with the guidelines of the National Institutes of Health. The study conformed to the Guidelines of the International Association for the Study of Pain.[26]

Experimental model of pain (CCI model)

At six weeks of age, mice were deeply anesthetized with intraperitoneal injection of 0.3 mg/kg body weight medetomidine (GEA ORION Farm Technologies Co, Ltd., Nagano, Japan), 4.0 mg/kg midazolam (Astellas Pharma Inc., Tokyo, Japan), and 5.0 mg/kg butorphanol (Meiji Seika Pharma Co., Ltd., Tokyo, Japan).[27] CCI mice were prepared using a modification of the procedure of Bennett and Xie.[28] Briefly, the sciatic nerve was exposed in the left mid-thigh, proximal to its trifurcation. Three ligatures of 4-0 chromic gut suture (Ethicon Inc., Bedminster Township, NJ, USA) were tied loosely around the sciatic nerve at about 1-mm intervals. Sham controls were subjected to the same surgical procedure, except that the sciatic nerve was undisturbed. For all groups, the overlying muscle was repositioned, and the skin was sutured closed with 4-0 silk.

Behavioral assessment

Behavioral tests were performed (CCI and GJG-treated CCI group, n = 8; Sham and GJG-treated Sham group, n = 5) at several time points (one day before surgery, and 3, 7, 14, 21 and 28 days after surgery). Animals were habituated to the tests for six days before surgery, and the pre-surgery baseline was measured one day before ligation of the sciatic nerve. Before drug evaluation, the mice underwent latency measurement and were allocated to groups to minimize the differences in average threshold among the groups. These tests were performed in a blinded fashion.

Mechanical allodynia (von Frey test). Mechanical allodynia was assessed according to the previously reported method of Sommer and Schafers,[29] using a series of von Frey filaments (0.6 to 10 g, Ugo Basile Biological Research Apparatus, Varese, Italy). Animals were placed in testing chambers consisting of clear plastic cylinders on a wire-mesh floor, which allowed them to move freely. They were acclimatized to this environment for 10 min prior to testing to allow for behavioral

accommodation. The von Frey filaments were applied to the midplantar surface of the hindpaw ipsilateral to the surgery through the mesh floor. The time interval between consecutive filament administrations was at least 3 s.[29] We employed the von Frey filaments according to the up-down method to obtain the baseline mechanical threshold. The response threshold was defined as the weakest-force filament application that prompted at least three positive responses in five trials according to the method described by Yalcin et al.[30]

Cold allodynia (cold-plate test). Cold allodynia was assessed according to the previously reported method of Bennett and Xie[28] using an electrically cooled and thermostatically controlled aluminum surface set to a temperature of $2^{\circ}C$ (Cold/Hot Plate Analgesia Meter; IITC Life Science, Woodland Hills, CA, USA). Mice were placed on the cold plate ($2^{\circ}C$) in a plexiglass container (20 cm wide, 10 cm deep, 40 cm high), and the latency time from the starting to the end point of either lifting, licking or shaking of the left hind paw (ipsilateral to the injury side) was measured.[31] A cut-off time of 30 s was used to prevent tissue damage in the cold-plate test. The latency of paw withdrawal from the cold stimulus was measured in five time trials, each separated by a 15-min interval, and the average latency was calculated from three of the five time trials, excluding the maximum and minimum values.

Thermal hyperalgesia (hot-plate test). Thermal hyperalgesia was assessed according to the previously reported method of Eddy and Leimbach[31] and Woolfe and Macdonald[32] using the Cold/Hot Plate Analgesia Meter (IITC Life Science). Mice were placed on the hot plate set to a temperature of $55 \pm 0.5^{\circ}C$. To minimize tissue damage, a cut-off time of 30 s was adopted. The latency of paw withdrawal from the heat stimulus was measured from the starting to the end point of jumping, shaking, or licking of the left hind paw.

Immunohistochemistry

Mice were sacrificed prior to collection of samples for immunohistochemical analysis at 1, 2, 3, or 7 days post-surgery (each group, n = 3). The spine including the lumbar spinal cord was removed and fixed by submersion in 10% neutral-buffered formalin for one week. Tissue was decalcified in ethylenediaminetetraacetic acid (EDTA) for four weeks. Decalcified tissues were then processed by dehydration through a gradient series of ethanol, cleared in xylene, and embedded in paraffin blocks using automatic processing and embedding equipment. Paraffin sections 4 μm in thickness were dewaxed using xylene and rehydrated in a descending alcohol series followed by distilled water. Following quenching of endogenous peroxidase with 1% hydrogen peroxide in methanol for 30 min, high temperature antigen retrieval was performed by immersion of the slides in a water bath at 95–98°C in 0.1 M trisodium citrate buffer pH 6.0 for 45 min.[33]

After quenching endogenous peroxidase activity in 1% H_2O_2 for 30 min, sections were washed with 1% Tris-buffered saline (TBS) for 15 min. Sections were incubated overnight at 4°C in primary antibodies: rabbit anti-Iba1 (1:100, Novus Biologicals, Littleton, CO, USA) and rabbit anti-TNF-α (1:25; Abcam, Cambridge, MA, USA). The sections were washed six times with 1% TBS (5 min each) and then incubated for 1 h at room temperature in secondary antibodies: Alexa 488-conjugated rabbit-IgG and Alexa 647-conjugated goat-IgG (1:1000; Invitrogen, Carlsbad, CA, USA). Immunohistochemical images were obtained using a confocal laser microscope (Leica TCS SP5 MP; Leica, Tokyo, Japan), and digital images were captured with LAS AF software (Leica).

Iba1 and TNF-α immunoreactivity was quantitatively determined by counting the number of positive cells in the spinal cord in a 10^4 μm^2 box placed on areas of the lateral, central, and medial superficial laminae of the dorsal horn using the nuclear marker DAPI to assist in determining positive cells, as described previously.[34] Cell counts were done within the gray matter of the dorsal horn in spinal segments ranging from L4 to L5. All images of Iba1 and TNF-α labeling were taken at the same time with the same camera settings. All samples were scored blind until analysis was complete.

Western blotting analysis

Samples for Western blotting analysis were obtained upon sacrifice of mice at one, three, or seven days post-surgery (each group, n = 3). The spinal cord (L4–L6) was removed and separated into ipsi- and contralateral halves under a mesoscope and then frozen at −80°C until use. The Western blot assay was conducted according to the method described by Hylden and Wilcox.[35] Briefly, tissue samples were homogenized in RIPA buffer containing 50 mM Tris-HCl (pH 7.6), 150 mM NaCl, 1% NP-40, 0.1% SDS and 0.5% each sodium deoxycholate and protease inhibitor cocktail (1×). Lysates were centrifuged at $14000 \times g$ for 10 min at 4°C. Protein was determined using the BCA Protein Assay Kit (Sigma Chemical, St. Louis, MO, USA). Spinal cord homogenates (10–20 μg protein) were separated using 15% SDS-polyacrylamide gel electrophoresis and then transferred to a PVDF membrane (Millipore, Billerica, MA, USA). After the blots were washed with TBS/T (25 mM Tris–HCl (pH 7.4), 137 mM NaCl, 2.68 mM KCl and 0.1 w/v% Tween 20), the membranes were blocked with 5% skim milk for 1 h, Blocking One® (Nacalai Tesque, Kyoto, Japan) for 20 min or Blocking

One-P® (Nacalai Tesque) for 20 min at room temperature. The membranes were then incubated at 4°C overnight with primary antibodies specific for Iba1 (goat polyclonal antibody [pAb], 1:1000; Novus Biologicals), phospho-p38 (rabbit pAb, 1:1000; Cell Signaling Technology Inc. (CST), Danvers, MA, USA), p38 (rabbit pAb, 1:1000; CST), TNF-α (rabbit pAb, 1:500; CST or goat pAb, 1:2000; R&B, Calabasas, CA, USA) or GAPDH (rabbit monoclonal antibody, 1:2000; CST). The membranes were incubated with horseradish peroxidase (HRP)-conjugated secondary anti-rabbit antibody (1:10000; Amersham Pharmacia Biotech Inc., Piscataway, NJ, USA), anti-mouse antibody (1:10000; Amersham Pharmacia Biotech Inc.) or anti-goat antibody (1:10000; Santa Cruz Biotechnology, Santa Cruz, CA, USA). Immunocomplexes were detected by chemiluminescence (Wako Pure Chemical Industries, Osaka, Japan) and visualized using a fluorimager system (Image Quant LAS 4000; GE Healthcare Life Sciences, Piscataway, NJ, USA). For densitometric analyses, the blots were quantified using Image Quant analysis software (GE Healthcare Life Sciences, Piscataway, NJ, USA). Results are expressed as the ratio of target gene immunoreactivity to GAPDH immunoreactivity.

Intrathecal injection of TNF-α

Intrathecal (i.t.) administration was performed in conscious mice according to the method of Hylden.[35,36] Before the experiment, we performed methylene blue dye tests to check the distribution consistency of the injected drug. The i.t. injection of 4 μl of 1% methylene blue was localized at L4–L5. The dye was distributed both rostrally and caudally within a short distance (about 1.0 to 1.5 cm); no dye was observed in the brain. We divided the CCI mice into four groups: CCI and GJG-treated CCI groups that were administered i.t. PBS, and CCI and GJG-treated CCI groups that were administered i.t. TNF-α (n = 4 per group). For these mice, 10 pg recombinant TNF-α (R&B, Calabasas, CA, USA) diluted with 4 μl PBS or PBS alone was i.t. injected at post-operative day 1. Behavioral tests were used to evaluate analgesic effects as described above. The areas under the time-course curves (AUC) in the cold-plate test were calculated using the trapezoidal rule.[37]

Statistical analysis

The obtained data are expressed as means ± SD. Data were analyzed with the Statistical Package for the Social Sciences (SPSS) version 22 (IBM, Tokyo, Japan) and JMP12 (SAS, Tokyo, Japan). The results of the behavioral study were analyzed using Tukey-Kramer's post hoc test following two-way repeated measures ANOVA. The results of immunoblot and immunochemical analyses were statistically analyzed using one-way ANOVA or Dunnett's test. A *p*-value of less than 0.05 was considered significant.

Results

GJG did not induce any significant adverse effects

All mice survived after the CCI or sham operation. No mice in the GJG group experienced side effects such as weight loss or unusual activity. No significant differences were found in daily food intake among the four groups (Sham, 2.8 ± 0.1 g/day; GJG-treated Sham, 2.6 ± 0.1 g/day; CCI, 2.8 ± 0.1 g/day; GJG-treated CCI, 2.6 ± 0.1 g/day, $p = 0.384$, one-way ANOVA.). The intake of GJG was largely the same between the GJG-fed groups (GJG-treated CCI, 0.1 ± 0.01 g/day; GJG-treated Sham, 0.1 ± 0.01 g/day; $p = 0.786$, one-way ANOVA). The increase in body weight over time was slightly lower in the GJG-fed groups; however, no significant differences among the four groups were noted (Sham, 0.19 ± 0.02 g/day; GJG-treated Sham, 0.19 ± 0.05 g/day; CCI, 0.18 ± 0.05 g/day; GJG-treated CCI, 0.18 ± 0.06 g/day; $p = 0.958$, one-way ANOVA). No other adverse effects were observed in the GJG-fed groups.

GJG attenuated CCI-induced allodynia and hyperalgesia

We measured the inhibitory effect of GJG on CCI-induced allodynia and hyperalgesia. Figure 2(a) to (c) shows the time-course of the von Frey, cold-plate and hot-plate tests. There were no significant differences among the experimental groups in baseline threshold before the surgery (von Frey test, 9 ± 1 g; cold-plate test, 30 s; hot-plate test, 8.3 ± 0.7 s; $p = 0.941$, one-way ANOVA). In the three nociception assays, the CCI groups showed apparent allodynia and hyperalgesia compared with the Sham groups (von Frey test, $p < 0.0001$; cold-plate test, $p < 0.0001$; hot-plate test, $p < 0.0001$; two-way repeated measures ANOVA; Figure 2(a) to (c)). The maximal effect of mechanical allodynia induced by the CCI operation was observed on day 14, which is consistent with previous reports.[28,38] GJG significantly improved the threshold of mechanical and cold allodynia compared with the CCI group (von Frey test, $p < 0.0001$; cold-plate test, $p < 0.0001$; two-way repeated measures ANOVA; Figure 2(a) and (b). In these nociception assays, the anti-allodynic effect of GJG was apparent from day 7 to day 28. In the hot-plate test, GJG significantly decreased the threshold for thermal hyperalgesia compared with the CCI group ($p = 0.011$, two-way repeated measures ANOVA, Figure 2(c)). Furthermore, the anti-hyperalgesic effect of GJG was observed from day 14 to day 28. GJG did not affect
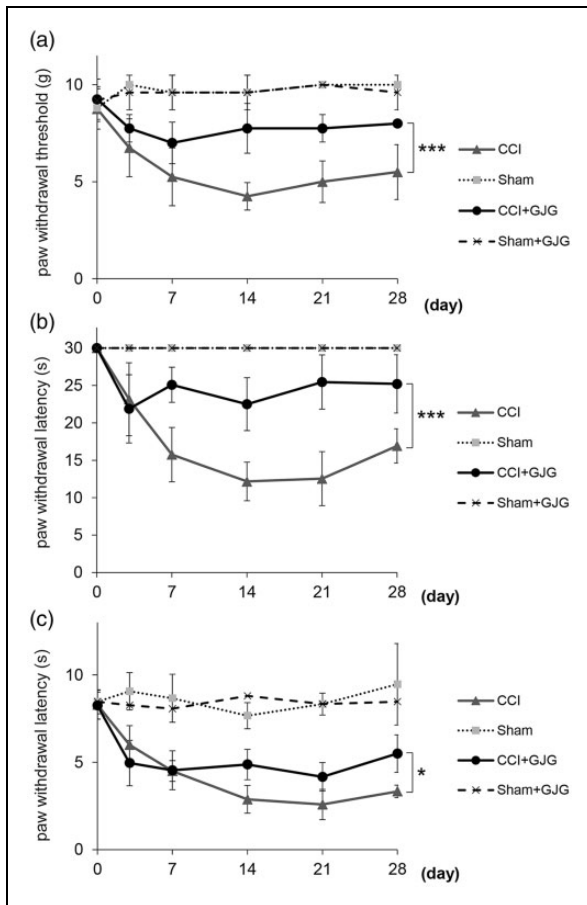
Figure 2. GJG administration attenuated CCI-induced allodynia and hyperalgesia as assessed by behavioral tests. (a) von Frey test (mechanical allodynia). (b) cold-plate test (cold allodynia). (c) hot-plate test (thermal hyperalgesia). Data are presented as means ± SD. Data were analyzed using two-way repeated measures ANOVA with Tukey's HSD post hoc analyses (***$p < 0.0001$ and *$p < 0.05$ indicate significant differences between the GJG-treated CCI group and the control CCI group, n = 5–8).

the behavioral response of the Sham-operated mice in any behavior test.

GJG inhibited CCI-induced spinal microglial activation

Because GJG improved the neuropathic behavior of CCI model mice in the early postoperative period, we focused our attention on microglia, a well-known factor in the establishment of NP, at the early phase in CCI model mice.[39] We investigated the activity of microglia in the dorsal horn using immunohistochemistry and Western blotting analysis. In immunohistochemical analysis, Iba1, a marker of activated microglia, was increased in the ipsilateral dorsal horn of CCI mice compared to Sham mice (Figure 3(a)). The expression of Iba1 peaked at day 3 in CCI mice and was decreased by GJG treatment. We confirmed the above results using

Western blotting analysis. Figure 3(b) shows that the Iba1 protein was increased at day 1 compared to that in Sham mice and peaked at day 3 in the ipsilateral spinal cord of CCI mice. Similar to the immunohistochemical results, GJG inhibited the expression of Iba1. Quantification of the Western blotting results indicated that GJG significantly decreased the expression of Iba1 at day 3, as shown in Figure 3(c) (CCI vs. GJG-treated CCI, $p = 0.0245$, Dunnett's test). These results suggested that GJG improved allodynia in CCI model mice via the suppression of microglial activity.

GJG suppressed the expression of TNF-α from activated microglia

Activated microglia are a well-known source of cytokines.[40] TNF-α secreted from activated microglia contributes to the pathogenesis of NP.[21] We therefore next investigated the expression of TNF-α in the dorsal horn using Western blotting analysis. Figure 4(a) shows the expression of TNF-α in the lumbar ipsilateral spinal cord. In CCI mice, TNF-α was increased from day 1 to day 3 and decreased at day 7 post-surgery compared to Sham mice. In GJG-treated CCI mice, the expression of TNF-α was decreased from day 1 to day 7 post-surgery compared to CCI mice. Quantification of Western blotting data as shown in Figure 4(b) indicated that TNF-α was significantly increased at day 1 and day 3 in CCI model mice compared to Sham mice (day 1, $p = 0.0444$; day 3, $p = 0.0041$, Sham vs. CCI, Dunnett's test) and that GJG significantly decreased TNF-α expression at day 1 post-surgery ($p = 0.032$, CCI vs. GJG-treated CCI, Dunnett's test). These results suggested that GJG inhibits the expression of TNF-α in activated microglia during the early stage in CCI model mice. Because TNF-α activates the signal transduction of p38 MAPK in microglia, we next investigated the expression of phospho-p38 and p38 in the ipsilateral spinal cord using Western blotting analysis.[41] Although the expression of p38 remained unchanged in the ipsilateral spinal cord, the phosphorylation of p38 was increased in CCI model mice compared to sham mice. GJG inhibited the upregulation of the phosphorylation of p38 from day 1 to day 7 in CCI mice (Figure 4(c)). Quantification of Western blotting data as shown in Figure 4(d) indicated that phospho-p38 was significantly increased at day 3 in CCI model mice compared to Sham mice ($p = 0.0003$, Sham vs. CCI, Dunnett's test) and that GJG significantly decreased phospho-p38 expression at day 3 post-surgery ($p = 0.0195$, CCI vs. GJG-treated CCI, Dunnett's test).

To determine whether activated microglia are the source of the TNF-α, we performed double staining immunohistochemistry for Iba1 and TNF-α in the ipsilateral dorsal horn of the lumbar spinal cord at postoperative day 3. Figure 5(a) shows that Iba1 and
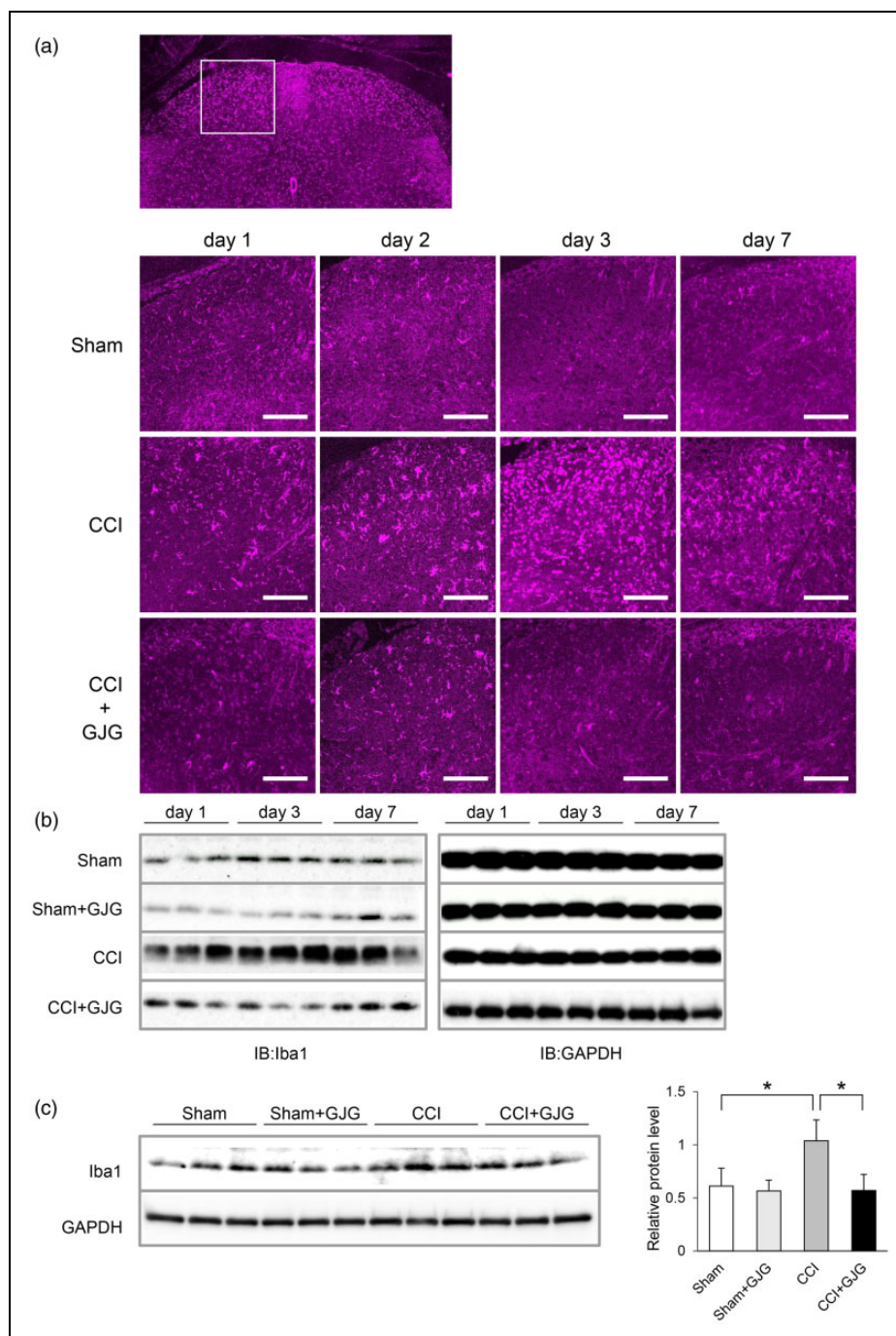
Figure 3. GJG inhibited the expression of Iba1, a microglial activation marker, in the ipsilateral dorsal horn. (a) Immunohistochemical analysis of Iba1 from day 1 to day 7 post-operation. Confocal images were taken at 40 × magnification. Magenta fluorescence indicates Iba1-positive cells. Scale bar = 100 μm. (b) Results of Western blotting analysis of Iba1 from day 1 to day 7 post-operation. GAPDH is shown as a loading control. (c) Quantification of Western blotting analysis of Iba1 in Sham, GJG-treated Sham, CCI, and GJG-treated CCI groups on day 3 post-operation. The left blot was densitometrically analyzed, and the ratio of Iba1 immunoreactivity to GAPDH immunoreactivity was determined. Each data point represents the mean ± SD. n = 3. Data were analyzed using Dunnett's test (*$p < 0.05$ indicates a significant difference between the indicated groups).

TNF-α were increased in CCI model mice compared to Sham mice and were decreased by GJG at day 3. The merged images of Iba1 and TNF-α showed that most of the TNF-α was expressed in Iba1-positive cells.

To quantify the above results, we calculated the percentage of TNF-α/Iba1-positive cells in each group of mice. TNF-α/Iba1-positive cells were significantly increased in the CCI group compared with the sham group (CCI,
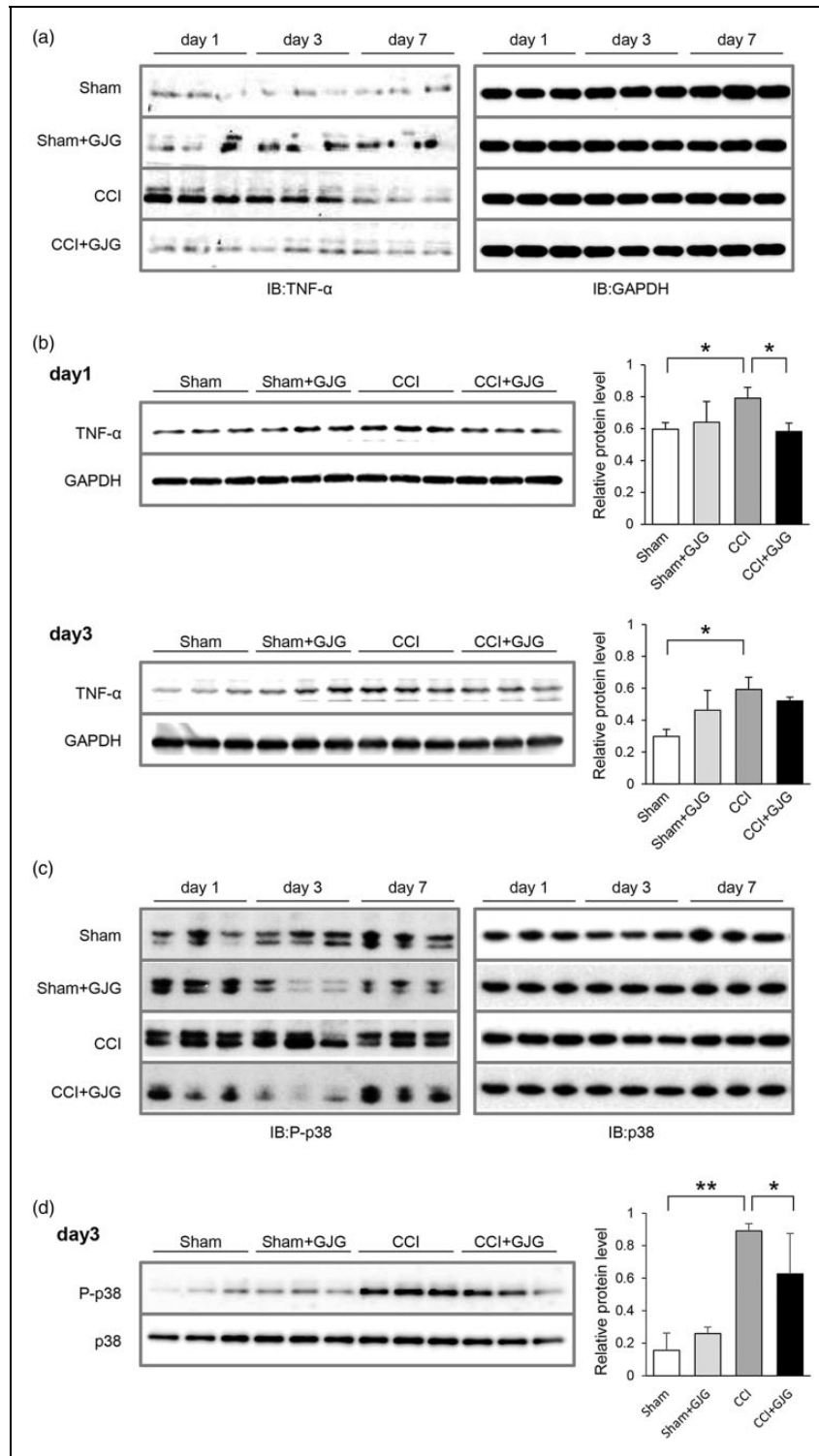
Figure 4. GJG inhibited the expression of TNF-α in the ipsilateral spinal cord. (a) Western blotting analysis of TNF-α in the lumbar ipsilateral spinal cord from day 1 to day 7 post-operation. The left panel shows TNF-α. GAPDH is shown at right as a loading control. (b) Quantification of Western blotting analysis of TNF-α in Sham, GJG-treated Sham, CCI, and GJG-treated CCI groups on day 1 (top panels) and day 3 (bottom panels) post-operation. The left blots were densitometrically analyzed, and the ratio of TNF-α immunoreactivity to GAPDH immunoreactivity was determined. Each data point represents the mean ± SD. n = 3. Data were analyzed using Dunnett's test (*$p < 0.05$ indicates a significant difference between the indicated groups). (c) Western blotting analysis of phospho-p38 and p38 MAPK expression in the ipsilateral spinal cord from day 1 to day 7 post-operation. (d) Quantification of Western blotting analysis of phospho-p38 in Sham, GJG-treated Sham, CCI, and GJG-treated CCI groups on day 3 post-operation. The left blots were densitometrically analyzed, and the ratio of phosho-p38 immunoreactivity to p38 immunoreactivity was determined. Each data point represents the mean ± SD. n = 3. Data were analyzed using Dunnett's test (**$p < 0.001$ and *$p < 0.05$ indicates a significant difference between the indicated groups.).
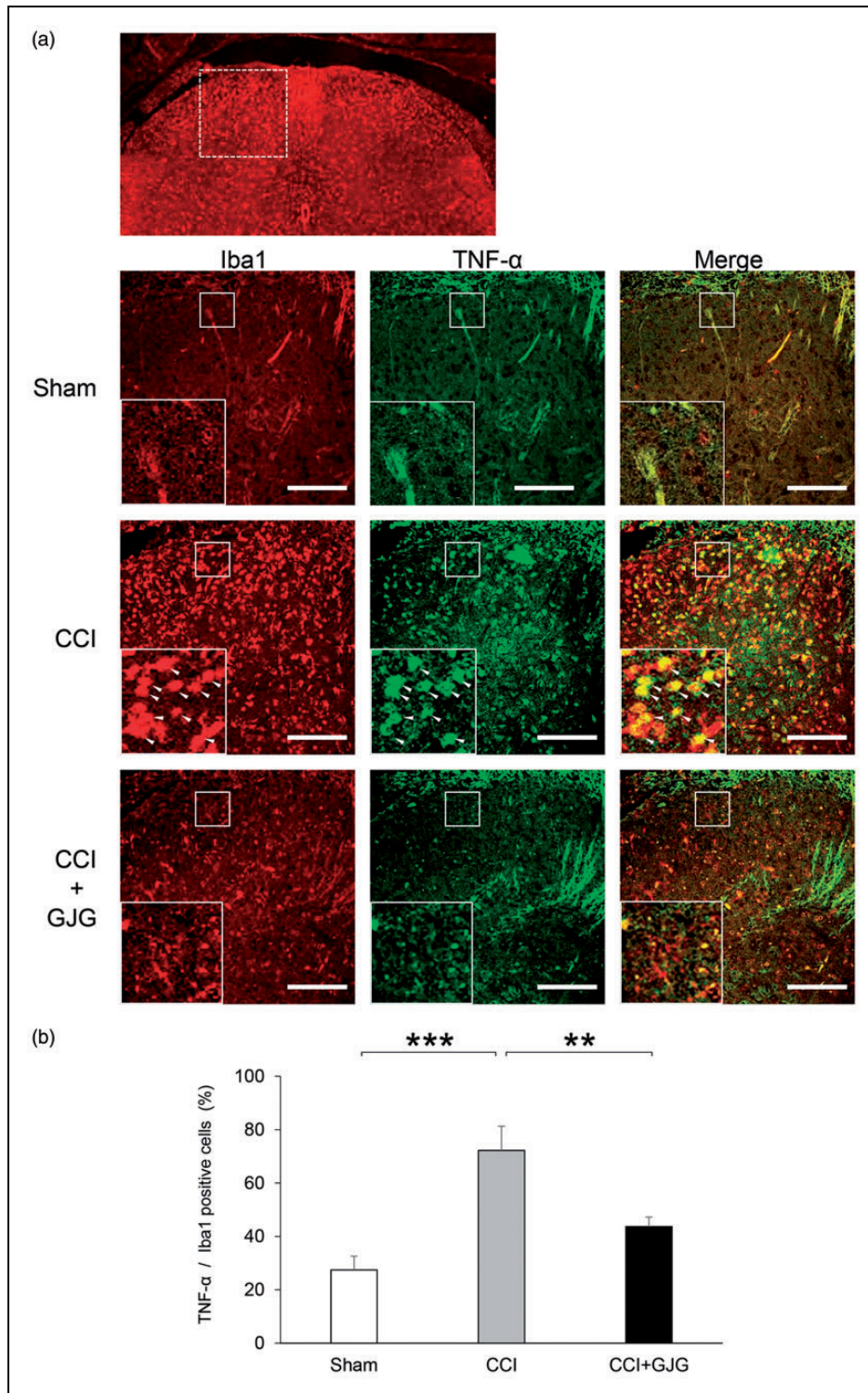
Figure 5. GJG inhibited the expression of TNF-α in Iba1-positive microglia in the ipsilateral dorsal horn. (a) Immunohistochemical images of Iba1 and TNF-α in the ipsilateral dorsal horn of the lumbar spinal cord on day 3 post-operation. Left panels show Iba1-positive cells (deep red). Middle panels show TNF-α-positive cells (green). Right panels showed merged images of Iba1 (deep red) and TNF-α (green). Merged images of double-stained cells indicated that TNF-α was localized in Iba1-positive cells (yellow). The white arrowheads indicate Iba1/TNF-α double-positive cells. Confocal images were taken at $40 \times$ magnification. Scale bar = 100 μm. (b) Histogram of the mean percentage value of the number of Iba1/TNF-α-positive cells in the superficial laminae of the ipsilateral dorsal horn in each mouse group. The average numbers of Iba1-positive cells/10^4 μm^2 were 14.7 ± 7.2 in Sham, 27.4 ± 3.7 in CCI and 22.2 ± 4.5 in CCI + GJG. The average numbers of both Iba1-positive and TNF-α-positive cells/10^4μm^2 were 3.9 ± 1.6 in Sham, 19.9 ± 4.2 in CCI and 9.7 ± 1.8 in CCI + GJG. Each data point represents the mean $\pm$ SD. Data were analyzed using one-way repeated measures ANOVA with Tukey's HSD post hoc analyses (***$p < 0.0001$ and **$p < 0.01$ indicates a significant difference between the Sham group versus the CCI group and between the CCI group versus the GJG-treated CCI group; n = 3).

72.2 ± 9.1%; Sham, 27.4 ± 5.1%, $p < 0.0001$, one-way ANOVA) and were significantly decreased in the GJG-treated CCI group compared to the CCI group (GJG-treated CCI, 43.7 ± 3.6%; $p = 0.008$, one-way ANOVA) (Figure 5(b)). These results indicated that GJG affects allodynia in CCI model mice via the suppression of TNF-α expression in activated microglia.

Intrathecal injection of TNF-α reversed the analgesic effect of GJG in cold allodynia

Finally, to confirm that the inhibitory effect of GJG in CCI model mice was mediated via the suppression of TNF-α expression in activated microglia, we examined whether i.t. administration of TNF-α abrogated the anti-allodynic effects of GJG in CCI model mice. We determined the appropriate i.t. dose of TNF-α by reference to previous reports of a TNF-α-induced NP model.[42,43] In the von Frey test, 10 pg TNF-α (i.t.) decreased the anti-allodynic effect of GJG, although not significantly ($p = 0.546$, i.t. TNF-α GJG-treated CCI vs. i.t. phosphate-buffered saline (PBS) GJG-treated CCI, two-way repeated measures ANOVA; Figure 6(a)). On the other hand, in the cold-plate test, 10 pg TNF-α (i.t.) significantly opposed the anti-allodynic effect of GJG (i.t. TNF-α GJG-treated CCI vs. i.t. PBS GJG-treated CCI, $p < 0.0001$; two-way repeated measures ANOVA, Figure 6(b)). Moreover, the significance of the effect of TNF-α on cold allodynia was higher for GJG-treated CCI mice ($p < 0.0001$ as mentioned above) than for non-GJG-treated CCI mice (i.t. TNF-α CCI vs. i.t. PBS CCI, $p = 0.044$; two-way repeated measures ANOVA, Figure 6(b)). The area under the effect-time curves (AUC) and significant differences in AUC values observed in the cold-plate test between the differently treated CCI mice are shown in Figure 6(c). The cold threshold in CCI mice was significantly increased by GJG treatment (i.t. PBS CCI vs. i.t. PBS GJG-treated CCI, $p < 0.0001$, one-way ANOVA) and was decreased by TNF-α administration (i.t. PBS CCI vs. i.t. TNF-α CCI, $p = 0.044$). The analgesic effects of GJG were opposed by i.t. TNF-α, and no significant difference was observed between the cold threshold of the i.t. TNF-α GJG-treated CCI group and that of the i.t. PBS CCI group ($p = 0.511$, one-way ANOVA). Figure 6(d) shows the synergistic interaction between TNF-α and GJG. One-way ANOVA indicated the statistical significance of this interaction between GJG and TNF-α ($p = 0.013$, Figure 6(d)).

Discussion

In the present study, we showed that GJG ameliorates allodynia and hyperalgesia in CCI model mice via the suppression of TNF-α expression from activated microglia in the spinal cord. GJG is a traditional Japanese herbal medicine approved for use in the elderly for treatment of lumbago, neuropathy, and related pathologies under Japan's National Health Insurance Program,[44] and these symptoms improve with GJG in clinical observation. Previous studies indicated that the mixture of several components that is found in Kampo medicine provides additive and/or synergistic effects during treatment.[45,46] GJG is composed of 10 crude drugs, each of which has several pharmacologic actions. For example, components of GJG such as *Rehmanniae radix*,[47,48] *Corni fructus*,[49,50] *Plantaginis semen*,[51] *Moutan cortex*,[52,53] and *Cinnamomi cortex*[54,55] have anti-inflammatory effects. *Achyranthis radix*[56,57] and *Aconite tuber*[58,59] have analgesic effects. *Cinnamomi cortex* also evokes spontaneous pain and induces heat and mechanical hyperalgesia.[60,61] However, co-administration of these 10 components as a clinical regimen is thought to result in the most suitable effects through additive and/or synergistic effects and a reduction in side effects. However, as the molecular mechanism of GJG remains unknown, the exact criteria for its use have not been established. We previously reported that GJG inhibits sarcopenia, the aging-associated weakening and volume loss of muscle, via improvement of mitochondrial function, insulin/insulin-like growth factor-1 signal transduction and suppression of TNF-α in muscle.[62] We hypothesized that GJG is effective against NP via repression of TNF-α in the spinal cord. Several animal models have been established for NP, allodynia, and hyperalgesia. We selected CCI model mice to examine the analgesic effect of GJG. Challa[63] and Dowdall et al.[64] reported that the CCI model produces significant responses to the von Frey test, hot-plate test, and cold-plate test, supporting its usefulness and appropriateness in pain investigations. In our study, the results of the behavioral tests in CCI model mice were very similar to those in previous reports.[28,38]

Microglia in the spinal cord proliferates rapidly and play a crucial role in NP development. In newborn rats, which have immature microglia, i.t. lipopolysaccharide (LPS) exposure fails to evoke the allodynia response observed in adult rats,[65] suggesting an essential role for functional microglia in the pathogenesis of NP. After nerve injury, activated microglia display morphological changes, such as an amoeboid shape and an increase in the number of microglial markers.[17,66,67] In the spinal cord, the expression of Iba1, a marker of activated microglial, increases rapidly, and this increase is already very prominent two days after spared nerve injury.[67] In our study, the expression pattern of Iba1 in the ipsilateral dorsal horn of CCI model mice concurred with previous reports.[40,67] Furthermore, we confirmed that GJG suppressed the expression of Iba1 from day 2 to day 7. These results supported the hypothesis that activated
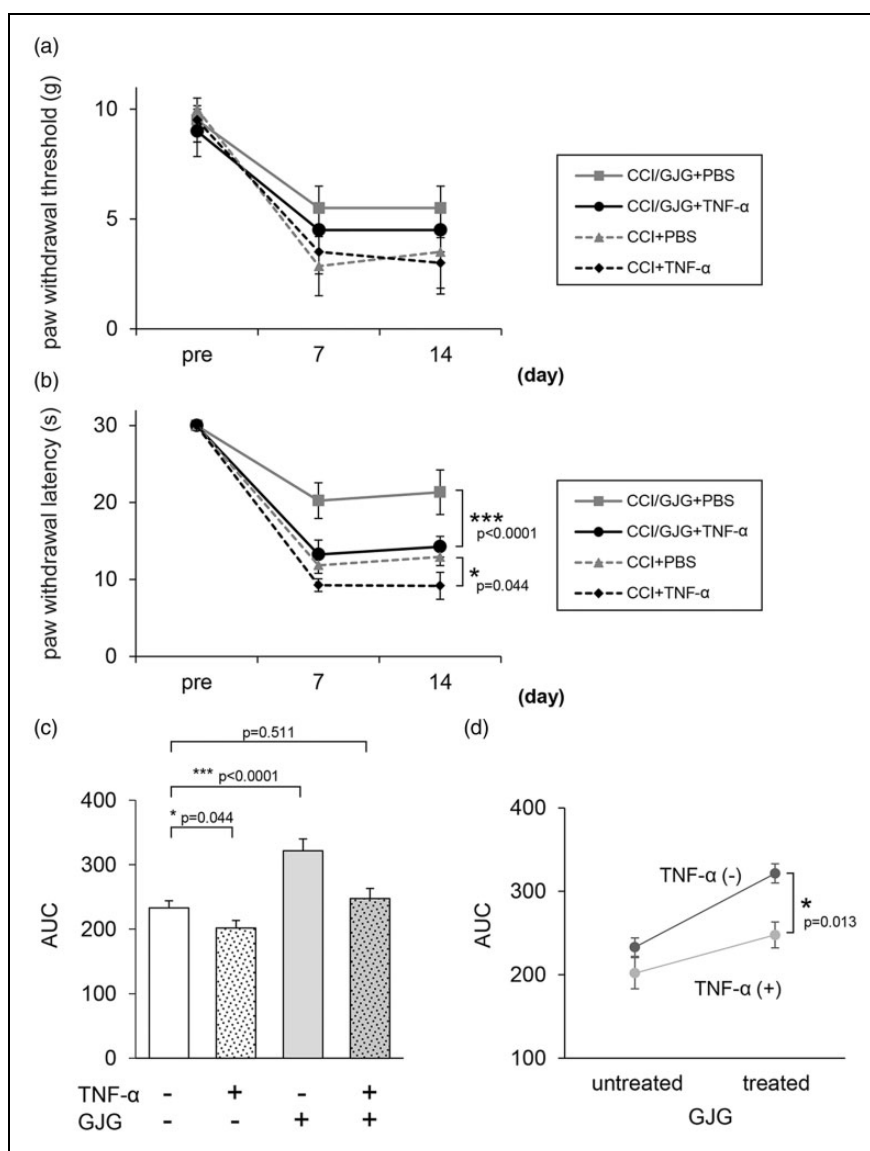
Figure 6. Intrathecal (i.t.) injection of TNF-α reversed the effects of GJG on cold allodynia. GJG was administered for two weeks to CCI model mice with i.t. TNF-α (10 pg) or with i.t. PBS. Pain behavior was assessed with the von Frey test (a) and the cold-plate test (b). The area under the effect-time curves (AUC) and significant differences between the AUC values for differently treated CCI mice in the cold-plate test were determined (c). Synergistic interaction between TNF-α and GJG in CCI mice in the cold-plate test (d). Data are presented as means $\pm$ SD. Data were analyzed using two-way repeated measures ANOVA or one-way repeated measures ANOVA (***$p < 0.0001$ and *$p < 0.05$ indicate a significant difference between the indicated groups. n = 4).

microglia are suppressed by GJG during the early phase of NP. We confirmed the correlation between the effect of GJG and the behavioral results seven days after the operation.

Microglia transforms into macrophage-like cells,[68] which express major histocompatibility complex antigens and secrete pro-inflammatory cytokines, e.g., TNF-α, interleukin-1, interleukin-6,[69,70] CCL2, CX3CL1,[71,72] and ATP.[73–75] TNF-α is a key cytokine in pro-inflammatory processes that involve necrosis, apoptosis, and proliferation.[20] Animal models of NP have consistently

indicated a pivotal role for TNF-α in both peripheral and central sensitization.[76] In NP, the role of TNF-α has been recognized at different levels of the nervous system, i.e., at the site of nerve injury, in dorsal root ganglion,[41] in the dorsal horn of the spinal cord,[77] and in the brain.[21] The central sensitization mechanism is mediated by TNF-α through glial systems in the dorsal horn of the spinal cord and brain.[21]

Given the aforementioned association between TNF-α and GJG, we further investigated the link between them by examining the effects of i.t. TNF-α

administration on GJG-treated CCI mice. Our results showed that TNF-α partially, but not significantly, attenuated the anti-allodynic effect of GJG in the von Frey test and significantly opposed the anti-allodynic effect of GJG in the cold-plate test. A previous report showed that i.t. injection of TNF-α into naïve mice results in peripheral hypersensitivity.[78] Our results showed that TNF-α-administered CCI mice showed more pain-related behavior than PBS-treated CCI mice (Figure 6(b)). TNF-α administration abrogated the previously observed positive effect of GJG on pain-related behavior compared to non-treated CCI mice (Figure 6(c) and (d)). This result indicated that TNF-α can inhibit the advantageous effects of GJG for NP and therefore that the effect of GJG on this NP model may be mediated via a TNF-α-related pathway.

To support our hypothesis that GJG improves NP via reduction of TNF-α expression, we performed an in vitro experiment using the mouse macrophage cell line, RAW264.7. We confirmed that GJG decreased the production of TNF-α from LPS-stimulated cells in a dose-dependent manner (see Supplemental data Materials and Methods, Figure 1S). This observation supports our hypothesis that GJG may reduce NP via reduction of TNF-α expression.

Substantial evidence shows that phospho-p38 MAPK can induce TNF-α production via NFκB in activated microglia and that subsequently, the animal shows more pain-related behavior.[21,22,79] In our study, GJG suppressed the phosphorylation of p38 that was induced in CCI mice, especially on day 3. By suppressing p38 phosphorylation in CCI mice, GJG likely exerted a positive effect on pain-related behavior via suppression of NFκB production. These results are consistent with other previous reports.[80] On the other hand, Moon et al.[81] reported that phospho-p38 is increased in astrocytes and neurons, but not in microglia on day 3 in CCI mice.[81] Further study is required to determine whether microglia and/or astrocytes affect pain via phospho-p38 MAPK function.

A close relationship between microglia and TNF-α has been reported.[40]TNF-α released from spinal microglia promotes further microglial activation[82] and accelerates the neuro-inflammatory process.[68,70–72,,80] Therefore, microglia can be identified as both a source and a target of TNF-α. Using merged, double-stained immunohistochemical images, our study demonstrated that Iba1 and TNF-α were co-expressed in the same cells, indicating that TNF-α is derived from microglia.

Furthermore, a causal link between TNF-α and the p38 MAPK system has been suggested.[40] p38 activation induces increased production of TNF-α, indicating that p38 promotes the inflammatory process. Conversely, inhibition of p38 prevents nucleocytoplasmic transport of TNF-α mRNA.[23] In our study, the phosphorylation of p38 was enhanced in CCI model mice compared to

sham mice. GJG suppressed p38 phosphorylation from day 1 to day 7 in the dorsal horn. These results indicate that GJG inhibited the neuro-inflammatory cascade in the spinal cord in CCI model mice.

In previous reports of NP models, TNF-α expression was characterized by an immediate increase following surgery, and peak levels were detected around 24 h,[43] sustained for about three days, and then decreased.[42,83] Iba1 was activated by CCI within 24 h and peaked between day 3 and day 7.[84] Phospho-p38 MAPK reached a peak on day 3, but was maintained at elevated levels even after three weeks.[85] These data are consistent with our results in which TNF-α was expressed from day 1 to day 3, and its expression was early and temporary compared to the more sustained expression of Iba1 or phospho-p38 MAPK. Phospho-p38 and microglia are also activated by factors other than TNF-α, such as interleukin-1β, CX3CR1, CCR2, P2X, and the P2Y12 receptor,[86] and microglia are additionally activated by factors such as erbB2, P2X4, and the CX3CR1 receptor.[87] These factors may be involved in the activation of microglia or phospho-p38 following CCI after the decrease in TNF-α expression. Our behavioral data showed that the development of allodynia and hyperalgesia tended to coincide roughly with the expression of TNF-α and that allodynia and hyperalgesia continued even after the decrease in TNF-α. These results indicated that pain persists due to various factors that are involved at various time points, which means that TNF-α is involved initially, and then subsequently other factors are involved, such as the activation of astrocytes or central sensitization in dorsal horn neurons.[2]

Because GJG is used to improve the symptoms caused by cold, or by excessive sensitivity to cold,[88] GJG may be involved in the mechanism by which cold is felt. In our study, GJG treatment resulted in a more significant improvement in cold allodynia than in other behavioral tests. In addition, the reversal of the behavioral effects of GJG by i.t. TNF-α was particularly marked for the effects of GJG on cold allodynia. Recently, the involvement of TRP channels has been noted in NP.[89] GJG suppresses functional alteration of TRP channels and TRPA1 and TRPM8 expression in oxaliplatin-induced peripheral neuropathy.[6,24] TRPA1 and TRPM8 in particular are mediators of cold allodynia. These reports suggest that GJG suppresses these TRP channels in CCI model mice. Notably, GJG is composed of 10 herbal medicines. We have already reported the results of 3DHPLC and LC/MS analysis of each herbal medicine.[62] Shibata et al.[59] reported that Aconite tuber, a constituent of GJG, inhibits astrocyte activation in the spinal cord of Seltzer model mice.[59] Thus, we cannot exclude the possibility that other pathways are involved in the analgesic effect of GJG. Hachimi-jio-gan, which contains less *Plantaginis semen* and *Achyranthis radix* than GJG, does not affect

paclitaxel-induced peripheral neuropathy.[90] The GJG components *Plantaginis semen* and *Achyranthis radix* may act synergistically, but further study is needed to clarify the anti-nociceptive effect of GJG.

In conclusion, our data supported the hypothesis that GJG ameliorates NP in CCI model mice. In the NP field, this is the first report demonstrating that GJG inhibits the expression of TNF-α derived from activated microglia. TNF-α inhibitors reduce NP.[91] However, anti-TNF therapies have several side effects, such as infections, infusion reactions, demyelination, interstitial pneumonia, and abnormalities in hepatic enzyme levels.[92] In contrast, GJG rarely exhibits severe adverse effects in CCI model mice or in humans.[14] For this reason, GJG may be suitable for the treatment of NP in the elderly and is a promising drug for the treatment of NP induced by neuro-inflammation.

Authors' contributions
MN mainly carried out experiments and analysis of this paper. NS performed histological preparations and technically assisted with Western blotting analysis. AN, YK, KB, and MS discussed experiments. HY supervised the experimental work. KH designed the study and coordinated the experimental work. All authors contributed to drafting of the work and to critical revision of the work for important intellectual content. All authors have approved the final version of the manuscript to be published and agree to be accountable for all aspects of the work in ensuring that questions related to the accuracy or integrity of any part of the work are appropriately investigated and resolved.

Declaration of Conflicting Interests
The author(s) declared the following potential conflicts of interest with respect to the research, authorship, and/or publication of this article: Keisuke Hagihara (2011-current) holds the position of an endowed chair in the Department of Kampo Medicine provided by Tsumura & Co., which produces the GJG. Miho Nakanishi, Yuki Kishida, and Kousuke Baba are members of the Department of Kampo Medicine.

Funding

References

1. Vos T, Flaxman AD, Naghavi M, et al. Years lived with disability (YLDs) for 1160 sequelae of 289 diseases and injuries 1990-2010: a systematic analysis for the Global Burden of Disease Study 2010. *Lancet* 2012; 380: 2163–2196.
2. Gilron I, Baron R and Jensen T. Neuropathic pain: principles of diagnosis and treatment. *Mayo Clin Proc* 2015; 90: 532–545.
3. Sommer C. Neuropathic pain: pathophysiology, assessment, and therapy. *Schmerz* 2013; 27: 619–32; quiz 33–34.
4. Finnerup NB, Attal N, Haroutounian S, et al. Pharmacotherapy for neuropathic pain in adults: a systematic review and meta-analysis. *Lancet Neurol* 2015; 14: 162–173.
5. Dworkin RH, O'Connor AB, Backonja M, et al. Pharmacologic management of neuropathic pain: evidence-based recommendations. *Pain* 2007; 132: 237–251.
6. Mizuno K, Kono T, Suzuki Y, et al. Goshajinkigan, a traditional Japanese medicine, prevents oxaliplatin-induced acute peripheral neuropathy by suppressing functional alteration of TRP channels in rat. *J Pharmacol Sci* 2014; 125: 91–98.
7. Pickering G. Analgesic use in the older person. *Curr Opin Support Palliat Care* 2012; 6: 207–212.
8. Tracy B and Sean Morrison R. Pain management in older adults. *Clin Ther* 2013; 35: 1659–1668.
9. Wong CS, Hui GK, Chung EK, et al. Diagnosis and management of neuropathic pain. *Pain Manage* 2014; 4: 221–231.
10. Mulla SM, Buckley DN, Moulin DE, et al. Management of chronic neuropathic pain: a protocol for a multiple treatment comparison meta-analysis of randomised controlled trials. *BMJ Open* 2014; 4: e006112.
11. Hui F, Boyle E, Vayda E, et al. A randomized controlled trial of a multifaceted integrated complementary-alternative therapy for chronic herpes zoster-related pain. *Altern Med Rev* 2012; 17: 57–68.
12. Usuki Y, Usuki S and Hommura S. Successful treatment of a senile diabetic woman with cataract with goshajinkigan. *Am J Chin Med* 1991; 19: 259–263.
13. Bahar MA, Andoh T, Ogura K, et al. Herbal medicine goshajinkigan prevents paclitaxel-induced mechanical allodynia without impairing antitumor activity of paclitaxel. *Evid Based Complement Alternat Med* 2013; 2013: 849754.
14. Kono T, Hata T, Morita S, et al. Goshajinkigan oxaliplatin neurotoxicity evaluation (GONE): a phase 2, multicenter, randomized, doubleblind, placebocontrolled trial of goshajinkigan to prevent oxaliplatininduced neuropathy. *Cancer Chemother Pharmacol* 2013; 72: 1283–1290.
15. Oki E, Emi Y, Kojima H, et al. Preventive effect of Goshajinkigan on peripheral neurotoxicity of FOLFOX therapy (GENIUS trial): a placebo-controlled, double-blind, randomized phase III study. *Int J Clin Oncol* 2015; 20: 767–775.

16. Yoshida N, Hosokawa T, Ishikawa T, et al. Efficacy of goshajinkigan for oxaliplatin-induced peripheral neuropathy in colorectal cancer patients. *J Oncol* 2013; 2013: 139740.

17. Tawata M, Kurihara A, Nitta K, et al. The effects of goshajinkigan, a herbal medicine, on subjective symptoms and vibratory threshold in patients with diabetic neuropathy. *Diabetes Res Clin Pract* 1994; 26: 121–128.

18. Nishizawa M, Sutherland WH and Nukada H. Goshajinki-gan (herbal medicine) in streptozocin-induced diabetic neuropathy. *J Neurol Sci* 1995; 132: 177–181.

19. Woolf CJ and Mannion RJ. Neuropathic pain: aetiology, symptoms, mechanisms, and management. *Lancet* 1999; 353: 1959–1964.

20. Varfolomeev EE and Ashkenazi A. Tumor necrosis factor: an apoptosis JuNKie? *Cell* 2004; 116: 491–497.

21. Leung L and Cahill CM. TNF-alpha and neuropathic pain – a review. *J Neuroinflammation* 2010; 7: 27.

22. Chen RW, Lu XC, Yao C, et al. PAN-811 provides neuroprotection against glutamate toxicity by suppressing activation of JNK and p38 MAPK. *Neurosci Lett* 2007; 422: 64–67.

23. Suzuki T, Hide I, Ido K, et al. Production and release of neuroprotective tumor necrosis factor by P2X7 receptor-activated microglia. *J Neurosci* 2004; 24: 1–7.

24. Kato Y, Tateai Y, Ohkubo M, et al. Gosha-jinki-gan reduced oxaliplatin-induced hypersensitivity to cold sensation and its effect would be related to suppression of the expression of TRPM8 and TRPA1 in rats. *Anticancer Drugs* 2014; 25: 39–43.

25. Matsumura Y, Yokoyama Y, Hirakawa H, et al. The prophylactic effects of a traditional Japanese medicine, goshajinkigan, on paclitaxel-induced peripheral neuropathy and its mechanism of action. *Mol Pain* 2014; 10: 61.

26. Zimmermann M. Ethical guidelines for investigations of experimental pain in conscious animals. *Pain* 1983; 16: 109–110.

27. Kawai S, Takagi Y, Kaneko S, et al. Effect of three types of mixed anesthetic agents alternate to ketamine in mice. *Exp Anim* 2011; 60: 481–487.

28. Bennett GJ and Xie YK. A peripheral mononeuropathy in rat that produces disorders of pain sensation like those seen in man. *Pain* 1988; 33: 87–107.

29. Sommer C and Schafers M. Painful mononeuropathy in C57BL/Wld mice with delayed wallerian degeneration: differential effects of cytokine production and nerve regeneration on thermal and mechanical hypersensitivity. *Brain Res* 1998; 784: 154–162.

30. Yalcin I, Tessier LH, Petit-Demouliere N, et al. Beta2-adrenoceptors are essential for desipramine, venlafaxine or reboxetine action in neuropathic pain. *Neurobiol Dis* 2009; 33: 386–394.

31. Eddy NB and Leimbach D. Synthetic analgesics. II. Dithienylbutenyl-and dithienylbutylamines. *J Pharmacol Experiment Therapeut* 1953; 107: 385–393.

32. Woolfe G and Macdonald AD. The evaluation of the analgesic action of pethidine hydrochloride (Demerol). *J Pharmacol Experiment Therapeut* 1944; 80: 300–307.

33. da Costa DS, Meotti FC, Andrade EL, et al. The involvement of the transient receptor potential A1 (TRPA1) in the maintenance of mechanical and cold hyperalgesia in persistent inflammation. *Pain* 2010; 148: 431–437.

34. Clark AK, Yip PK, Grist J, et al. Inhibition of spinal microglial cathepsin S for the reversal of neuropathic pain. *Proc Natl Acad Sci U S A* 2007; 104: 10655–10660.

35. Hylden JL and Wilcox GL. Intrathecal substance P elicits a caudally-directed biting and scratching behavior in mice. *Brain Res* 1981; 217: 212–215.

36. Hylden JL and Wilcox GL. Intrathecal morphine in mice: a new technique. *Eur J Pharmacol* 1980; 67: 313–316.

37. Kayser V, Aubel B, Hamon M, et al. The antimigraine 5-HT 1B/1D receptor agonists, sumatriptan, zolmitriptan and dihydroergotamine, attenuate pain-related behaviour in a rat model of trigeminal neuropathic pain. *Br J Pharmacol* 2002; 137: 1287–1297.

38. Hogan Q. Animal pain models. *Reg Anesth Pain Med* 2002; 27: 385–401.

39. Mika J, Zychowska M, Popiolek-Barczyk K, et al. Importance of glial activation in neuropathic pain. *Eur J Pharmacol* 2013; 716: 106–119.

40. Hanisch UK. Microglia as a source and target of cytokines. *Glia* 2002; 40: 140–155.

41. Schafers M, Svensson CI, Sommer C, et al. Tumor necrosis factor-alpha induces mechanical allodynia after spinal nerve ligation by activation of p38 MAPK in primary sensory neurons. *J Neurosci* 2003; 23: 2517–2521.

42. Shubayev VI and Myers RR. Upregulation and interaction of TNFalpha and gelatinases A and B in painful peripheral nerve injury. *Brain Res* 2000; 855: 83–89.

43. Uceyler N, Tscharke A and Sommer C. Early cytokine gene expression in mouse CNS after peripheral nerve lesion. *Neurosci Lett* 2008; 436: 259–264.

44. TSUMURA&CO. Trends in pharmaceutical Kampo products sales and profits. *Annual Report* 2014, http://www.tsumura.co.jp/English/ir/library/annual/index.htm.

45. Motoo Y, Seki T and Tsutani K. Traditional Japanese medicine, Kampo: its history and current status. *Chin J Integr Med* 2011; 17: 85–87.

46. Zhang Q, Iwami D, Aramaki O, et al. Prolonged survival of fully mismatched cardiac allografts and generation of regulatory cells by Sairei-to, a Japanese herbal medicine. *Transplantation* 2009; 87: 1787–1791.

47. Wu PS, Wu SJ, Tsai YH, et al. Hot water extracted Lycium barbarum and Rehmannia glutinosa inhibit liver inflammation and fibrosis in rats. *Am J Chin Med* 2011; 39: 1173–1191.

48. Liu CL, Cheng L, Ko CH, et al. Bioassay-guided isolation of anti-inflammatory components from the root of Rehmannia glutinosa and its underlying mechanism via inhibition of iNOS pathway. *J Ethnopharmacol* 2012; 143: 867–875.

49. Park CH, Tanaka T and Yokozawa T. Anti-diabetic action of 7-O-galloyl-D-sedoheptulose, a polyphenol from Corni Fructus, through ameliorating inflammation and inflammation-related oxidative stress in the pancreas of type 2 diabetics. *Biol Pharm Bull* 2013; 36: 723–732.

50. Park CH, Noh JS, Kim JH, et al. Evaluation of morroniside, iridoid glycoside from Corni Fructus, on diabetes-induced alterations such as oxidative stress, inflammation, and apoptosis in the liver of type 2 diabetic db/db mice. *Biol Pharm Bull* 2011; 34: 1559–1565.

51. Chiu CS, Deng JS, Chang HY, et al. Antioxidant and anti-inflammatory properties of Taiwanese yam (Dioscorea japonica Thunb. var. pseudojaponica (Hayata) Yamam.) and its reference compounds. *Food Chem* 2013; 141: 1087–1096.

52. Fu PK, Yang CY, Tsai TH, et al. Moutan cortex radicis improves lipopolysaccharide-induced acute lung injury in rats through anti-inflammation. *Phytomedicine* 2012; 19: 1206–1215.

53. Zhang MH, Feng L, Zhu MM, et al. The anti-inflammation effect of Moutan Cortex on advanced glycation end products-induced rat mesangial cells dysfunction and High-glucose-fat diet and streptozotocin-induced diabetic nephropathy rats. *J Ethnopharmacol* 2014; 151: 591–600.

54. Liao JC, Deng JS, Chiu CS, et al. Anti-Inflammatory activities of Cinnamomum cassia constituents in vitro and in vivo. *Evid Based Complement Alternat Med* 2012; 2012: 429320.

55. Kubo M, Ma S, Wu J, et al. Anti-inflammatory activities of 70% methanolic extract from Cinnamomi Cortex. *Biol Pharm Bull* 1996; 19: 1041–1045.

56. Yu S, Wang C, Cheng Q, et al. An active component of Achyranthes bidentata polypeptides provides neuroprotection through inhibition of mitochondrial-dependent apoptotic pathway in cultured neurons and in animal models of cerebral ischemia. *PloS One* 2014; 9: e109923.

57. Yuan Y, Shen H, Yao J, et al. The protective effects of Achyranthes bidentata polypeptides in an experimental model of mouse sciatic nerve crush injury. *Brain Res Bull* 2010; 81: 25–32.

58. Suzuki T, Miyamoto K, Yokoyama N, et al. Processed aconite root and its active ingredient neoline may alleviate oxaliplatin-induced peripheral neuropathic pain. *J Ethnopharmacol* 2016; 186: 44–52.

59. Shibata K, Sugawara T, Fujishita K, et al. The astrocyte-targeted therapy by Bushi for the neuropathic pain in mice. *PloS One* 2011; 6: e23510.

60. Namer B, Seifert F, Handwerker HO, et al. TRPA1 and TRPM8 activation in humans: effects of cinnamaldehyde and menthol. *Neuroreport* 2005; 16: 955–959.

61. Tsagareli MG, Tsiklauri N, Zanotto KL, et al. Behavioral evidence of thermal hyperalgesia and mechanical allodynia induced by intradermal cinnamaldehyde in rats. *Neurosci Lett* 2010; 473: 233–236.

62. Kishida Y, Kagawa S, Arimitsu J, et al. Go-sha-jinki-Gan (GJG), a traditional Japanese herbal medicine, protects against sarcopenia in senescence-accelerated mice. *Phytomedicine* 2015; 22: 16–22.

63. Challa SR. Surgical animal models of neuropathic pain: pros and cons. *Int J Neurosci* 2014; 125: 170–174.

64. Dowdall T, Robinson I and Meert TF. Comparison of five different rat models of peripheral nerve injury. *Pharmacol Biochem Behav* 2005; 80: 93–108.

65. Moss A, Beggs S, Vega-Avelaira D, et al. Spinal microglia and neuropathic pain in young rats. *Pain* 2007; 128: 215–224.

66. Hanisch UK and Kettenmann H. Microglia: active sensor and versatile effector cells in the normal and pathologic brain. *Nat Neurosci* 2007; 10: 1387–1394.

67. Suter MR, Wen YR, Decosterd I, et al. Do glial cells control pain? *Neuron Glia Biol* 2007; 3: 255–268.

68. Vilhardt F. Microglia: phagocyte and glia cell. *Int J Biochem Cell Biol* 2005; 37: 17–21.

69. Ren K and Dubner R. Neuron-glia crosstalk gets serious: role in pain hypersensitivity. *Curr Opin Anaesthesiol* 2008; 21: 570–579.

70. Watkins LR and Maier SF. Glia: a novel drug discovery target for clinical pain. *Nat Rev Drug Discov* 2003; 2: 973–985.

71. Abbadie C, Bhangoo S, De Koninck Y, et al. Chemokines and pain mechanisms. *Brain Res Rev* 2009; 60: 125–134.

72. White FA, Jung H and Miller RJ. Chemokines and the pathophysiology of neuropathic pain. *Proc Natl Acad Sci U S A* 2007; 104: 20151–20158.

73. Inoue K, Tsuda M and Koizumi S. ATP- and adenosine-mediated signaling in the central nervous system: chronic pain and microglia: involvement of the ATP receptor P2X4. *J Pharmacol Sci* 2004; 94: 112–114.

74. Inoue K, Tsuda M and Koizumi S. Chronic pain and microglia: the role of ATP. *Novartis Found Symp* 2004; 261: 55–64; discussion: 64–67, 149–54.

75. Tsuda M and Inoue K. Neuropathic pain and ATP receptors in spinal microglia. *Brain Nerve* 2007; 59: 953–959.

76. Campbell JN and Meyer RA. Mechanisms of neuropathic pain. *Neuron* 2006; 52: 77–92.

77. Hashizume H, DeLeo JA, Colburn RW, et al. Spinal glial activation and cytokine expression after lumbar root injury in the rat. *Spine* 2000; 25: 1206–1217.

78. Gao YJ, Zhang L, Samad OA, et al. JNK-induced MCP-1 production in spinal cord astrocytes contributes to central sensitization and neuropathic pain. *J Neurosci* 2009; 29: 4096–4108.

79. Tsuda M, Mizokoshi A, Shigemoto-Mogami Y, et al. Activation of p38 mitogen-activated protein kinase in spinal hyperactive microglia contributes to pain hypersensitivity following peripheral nerve injury. *Glia* 2004; 45: 89–95.

80. Svensson CI, Schafers M, Jones TL, et al. Spinal blockade of TNF blocks spinal nerve ligation-induced increases in spinal P-p38. *Neurosci Lett* 2005; 379: 209–213.

81. Moon JY, Roh DH, Yoon SY, et al. sigma1 receptors activate astrocytes via p38 MAPK phosphorylation leading to the development of mechanical allodynia in a mouse model of neuropathic pain. *Br J Pharmacol* 2014; 171: 5881–5897.

82. Kuno R, Wang J, Kawanokuchi J, et al. Autocrine activation of microglia by tumor necrosis factor-alpha. *J Neuroimmunol* 2005; 162: 89–96.

83. Chung MK, Lee H, Mizuno A, et al. 2-aminoethoxydiphenyl borate activates and sensitizes the heat-gated ion channel TRPV3. *J Neurosci* 2004; 24: 5177–5182.

84. Zarpelon AC, Rodrigues FC, Lopes AH, et al. Spinal cord oligodendrocyte-derived alarmin IL-33 mediates neuropathic pain. *FASEB J* 2016; 30: 54–65.

85. Jin SX, Zhuang ZY, Woolf CJ, et al. p38 mitogen-activated protein kinase is activated after a spinal nerve ligation in spinal cord microglia and dorsal root ganglion neurons and contributes to the generation of neuropathic pain. *J Neurosci* 2003; 23: 4017–4022.

86. Bellei B, Mastrofrancesco A, Briganti S, et al. Ultraviolet A induced modulation of gap junctional intercellular communication by P38 MAPK activation in human keratinocytes. *Exp Dermatol* 2008; 17: 115–124.

87. Ren K and Dubner R. Interactions between the immune and nervous systems in pain. *Nat Med* 2010; 16: 1267–1276.

88. Yagi H, Sato R, Nishio K, et al. Clinical efficacy and tolerability of two Japanese traditional herbal medicines, Hachimi-jio-gan and Gosha-jinki-gan, for lower urinary tract symptoms with cold sensitivity. *J Tradit Complement Med* 2015; 5: 258–261.

89. Mandadi S, Hong P, Dhoopar AS, et al. Control of neonatal spinal networks by nociceptors: a potential role for TRP channel based therapies. *J Pharm Pharm Sci* 2013; 16: 313–320.

90. Andoh T, Kitamura R, Fushimi H, et al. Effects of goshajinkigan, hachimijiogan, and rokumigan on mechanical allodynia induced by Paclitaxel in mice. *J Tradit Complement Med* 2014; 4: 293–297.

91. Sommer C, Lindenlaub T, Teuteberg P, et al. Anti-TNF-neutralizing antibodies reduce pain-related behavior in two different mouse models of painful mononeuropathy. *Brain Res* 2001; 913: 86–89.

92. Nanau RM and Neuman MG. Safety of anti-tumor necrosis factor therapies in arthritis patients. *J Pharm Pharm Sci* 2014; 17: 324–361.